Regions of Strong Coupling Between Soil Moisture and Precipitation
Randal D. Koster *et al.*
Science **305**, 1138 (2004);
DOI: 10.1126/science.1100217

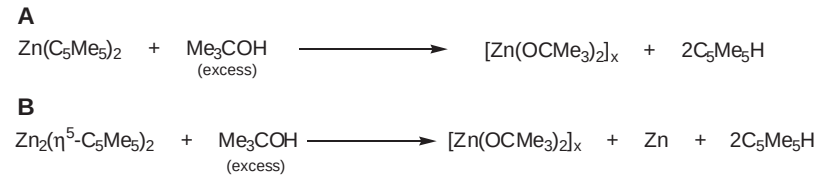

Fig. 4. Reactions of $Zn(C_5Me_5)_2$ (**A**) and $Zn_2(\eta^5\text{-}C_5Me_5)_2$ (**B**) with Me_3COH.

The alkoxide has been additionally identified by comparison of its infrared, ^1H, and $^{13}C\{^1H\}$ NMR spectra with those of an authentic sample prepared from $Zn(C_2H_5)_2$ and Me_3COH (*22*).

The synthesis of compound **1** suggests that related complexes of Cd and Hg could be isolated. It also seems plausible that the stabilization of the $[Zn–Zn]^{2+}$ unit does not require the existence of Zn–C bonds, which means that classical coordination compounds of the Zn_2^{2+} central unit are reasonable targets for future synthetic and structural studies.

References and Notes

1. F. A. Cotton, G. Wilkinson, C. A. Murillo, M. Bochmann, *Advanced Inorganic Chemistry* (Wiley, New York, ed. 6, 1999), chap. 15.
2. N. Wiberg, Ed., *Holleman-Wiberg Inorganic Chemistry* (Academic Press, New York, ed. 34, 2001), chap. XXIII.
3. R. Faggiani, R. J. Gillespie, J. E. Vekris, *J. Chem. Soc. Chem. Commun.* **1986**, 517 (1986).
4. D. L. Reger, S. S. Mason, *J. Am. Chem. Soc.* **115**, 10406 (1993).
5. D. H. Kerridge, S. A. Tariq, *J. Chem. Soc. A* **1967**, 1122 (1967).
6. F. Rittner, A. Seidel, B. Boddenberg, *Micropor. Mesopor. Mat.* **24**, 127 (1998).
7. Y. Tian, G. D. Li, J. S. Chen, *J. Am. Chem. Soc.* **125**, 6622 (2003).
8. P. O'Brien, in *Comprehensive Organometallic Chemistry II*, G. Wilkinson, F. G. A. Stone, E. Abel, Eds. (Pergamon, Oxford, UK, 1995), vol. 3, chap. 4.
9. J. T. B. H. Jastrzebski, J. Boersma, G. van Koten, W. J. J. Smeets, A. L. Spek, *Recl. Trav. Chim. Pays-Bas* **107**, 263 (1988).
10. R. Blom *et al.*, *Acta Chem. Scand. A* **40**, 113 (1986).
11. Data were identified by x-ray powder diffraction.
12. Materials and methods are available as supporting material on *Science* Online.
13. Two x-ray crystallographic analyses were carried out. The first made use of Bruker-Siemens Smart 1K charge-coupled device (CCD) diffractometer with a graphite monochromated Mo-K_α ($\lambda = 0.71073$ Å) radiation. Crystal data for **1** was as follows: $C_{20}H_{30}Zn_2$; molecular weight = 401.18; triclinic; space group $P\bar{1}$; $Z = 2$; T 173 (±2) K; a = 6.9329 (±3) Å, b = 10.8831 (±5) Å, c = 13.8384 (±7) Å, α = 109.777 (±1)°, β = 101.603 (±1)°, γ = 94.201 (±1)°, and V = 951.09 (±8) Å^3; goodness of fit = 0.988; R1[$I > 2\sigma(I)$] = 0.031; wR2 = 0.076 (all data). Atomic coordinates, bond lengths, and angles and other important parameters have been deposited with the Cambridge Crystallographic Data Centre as supplementary publication CCDC 233010. Details of the x-ray crystallographic analysis are also available on *Science* Online. The second analysis was carried out at –173°C (100 K), with the use of Cu-K_α ($\lambda = 1.54184$ Å) radiation, on a Bruker Smart 6000 CCD system equipped with a rotating anode. The results of the two determinations are very similar. Data from the second analysis can be obtained from the authors, upon request.
14. A compound initially formulated as $Co_2(\eta^5\text{-}C_5Me_5)_2$ by J. J. Schneider, R. Goddard, S. Werner, and C. Krüger [*Angew. Chem. Int. Ed. Engl.* **30**, 1124 (1991)] was subsequently shown to be $Co_2(\eta^5\text{-}C_5Me_5)_2(\mu\text{-}H)_3$[20].
15. J. L. Kersten *et al.*, *Angew. Chem. Int. Ed. Engl.* **31**, 1341 (1992).
16. P. Jutzi, N. Burford, *Chem. Rev.* **99**, 969 (1999).
17. L. Pauling, *The Nature of the Chemical Bond* (Cornell Univ. Press, Ithaca, NY, ed. 3, 1960), chap. 7.
18. E. Dorn, *J. Chem. Soc. Chem. Commun.* **1971**, 466 (1971).
19. H. Hao *et al.*, *Chem. Commun.* **2001**, 1118 (2001), and references therein.
20. In this refinement, the data with large 2θ angles were given higher weights, followed by a difference electron density synthesis with reflections with sinθ/λ.
21. R. Han, I. B. Gorrell, A. G. Looney, G. Parkin, *J. Chem. Soc. Chem. Commun.* **1991**, 717 (1991).
22. G. E. Coates, P. D. Roberts, *J. Chem. Soc. A* **1967**, 1233 (1967).

23. In memoriam of Professor Roberto Fernández de Caleya. We thank A. Justo (x-ray powder diffraction), M. A. Avilés (Raman spectra), and R. Fernández for their valuable help, and R. A. Andersen (University of California, Berkeley) for obtaining the mass spectrum of compound **1**. Supported by the Ministry of Science and Technology of Spain (to E.C., Project BQU2001-1995; and to I.R. for a research studentship).

Supporting Online Material

www.sciencemag.org/cgi/content/full/305/5687/1136/DC1
Materials and Methods
Tables S1 to S4
References

14 June 2004; accepted 7 July 2004

Regions of Strong Coupling Between Soil Moisture and Precipitation

The GLACE Team: Randal D. Koster,[1]* Paul A. Dirmeyer,[2] Zhichang Guo,[2] Gordon Bonan,[3] Edmond Chan,[4] Peter Cox,[5] C. T. Gordon,[6] Shinjiro Kanae,[7] Eva Kowalczyk,[8] David Lawrence,[9] Ping Liu,[10] Cheng-Hsuan Lu,[11] Sergey Malyshev,[12] Bryant McAvaney,[13] Ken Mitchell,[11] David Mocko,[10] Taikan Oki,[14] Keith Oleson,[3] Andrew Pitman,[15] Y. C. Sud,[1] Christopher M. Taylor,[16] Diana Verseghy,[4] Ratko Vasic,[17] Yongkang Xue,[17] Tomohito Yamada[14]

Previous estimates of land-atmosphere interaction (the impact of soil moisture on precipitation) have been limited by a lack of observational data and by the model dependence of computational estimates. To counter the second limitation, a dozen climate-modeling groups have recently performed the same highly controlled numerical experiment as part of a coordinated comparison project. This allows a multimodel estimation of the regions on Earth where precipitation is affected by soil moisture anomalies during Northern Hemisphere summer. Potential benefits of this estimation may include improved seasonal rainfall forecasts.

Atmospheric chaos severely limits the predictability of precipitation on seasonal time scales. Weather forecasts, which rely heavily on atmospheric initialization, rarely demonstrate skill beyond about a week. Hope for accurate seasonal forecasts lies with simulating the atmospheric response to slowly varying states of the ocean and land surface—components of the Earth system that can be predicted weeks to months in advance. A systematic response of the atmosphere to these boundary components would contribute skill to seasonal prediction.

The critical importance of the ocean surface in this regard is well known (*1*). Ocean temperature anomalies can be predicted a year or more in advance (*2*). Furthermore, the atmosphere responds particularly strongly (and predictably) to ocean temperature anomalies in certain regions—in "hot spots" of ocean-atmosphere coupling. The eastern equatorial Pacific is

[1]NASA Goddard Space Flight Center, Greenbelt, MD 20771, USA. [2]Center for Ocean-Land-Atmosphere Studies, Calverton, MD 20705, USA. [3]National Center for Atmospheric Research, Boulder, CO 80307, USA. [4]Meteorological Service of Canada, Toronto, Ontario M34 5T4, Canada. [5]Hadley Centre for Climate Prediction and Research, Exeter EX1 3PB, UK. [6]Geophysical Fluid Dynamics Laboratory, Princeton, NJ 08542, USA. [7]Research Institute for Humanity and Nature, Kyoto 602-0878, Japan. [8]CSIRO Atmospheric Research, Aspendale, Victoria 3195, Australia. [9]University of Reading, Reading, Berkshire RG6 6BB, UK. [10]Science Applications International Corporation, Beltsville, MD 20705, USA. [11]National Center for Environmental Prediction, Camps Springs, MD 20746, USA. [12]Princeton University, Princeton, NJ 08544, USA. [13]Bureau of Meteorology Research Centre, Melbourne, Victoria 3001, Australia. [14]University of Tokyo, Tokyo 153-8505, Japan. [15]Macquarie University, North Ryde, New South Wales 2109, Australia. [16]Centre for Ecology and Hydrology, Wallingford, Oxfordshire OX10 8BB, UK. [17]University of California, Los Angeles, CA 90095, USA.

*To whom correspondence should be addressed. E-mail: randal.d.koster@nasa.gov

the most famous oceanic hot spot, playing a key role in the El Niño–La Niña cycle (*3*).

Another potentially useful slowly varying component of the Earth system is soil moisture, which can influence weather through its impact on evaporation and other surface energy fluxes. Soil moisture anomalies can persist for months (*4*), and although a paucity of observations prevents an unambiguous demonstration of soil moisture impacts on precipitation (*5*), such impacts are often seen in atmospheric general circulation model (AGCM) studies (*6*, *7*). Indeed, some AGCM studies suggest that in continental midlatitudes during summer, oceanic impacts on precipitation are small relative to soil moisture impacts (*8*).

This suggests a question: Are there specific locations on the Earth's surface for which soil moisture anomalies have a substantial impact on precipitation? The identification of such hot spots would have important implications for the design of seasonal prediction systems and for the associated development of ground-based and satellite-based strategies for monitoring soil moisture, if such impacts were found to be local. In a broader sense, such identification is critical for understanding Earth's climate system and the limits of predictability therein.

Although AGCM studies (*9*–*12*) and even numerical weather prediction model studies (*13*) have addressed this question, published results are based on different experimental designs and reflect distinctive features of different model parameterizations. The coupling question, however, was recently addressed en masse by a dozen AGCM groups (*14*), all performing the same highly controlled numerical experiment. The experiments were coordinated by GLACE, the Global Land-Atmosphere Coupling Experiment (*15*). Each model contributing to GLACE generated several ensembles of boreal summer (June through August) simulations designed to quantify that model's land-atmosphere coupling strength (*16*) for that season. By combining the results across these models, we eliminate much of the undesired individual model dependence. We obtain, in effect, a unique result: a multimodel average depiction of the global distribution of land-atmosphere coupling strength. Given the limitations of the observational data, both now and in the foreseeable future, such a multimodel estimate of coupling strength distribution is arguably the best estimate attainable.

Each GLACE participant performed an ensemble of 16 simulations in which soil moisture varied between the simulations, and another ensemble in which the geographically varying time series of subsurface soil moisture was forced to be the same across the 16 simulations (*17*). Coupling strength—the degree to which all prescribed boundary conditions affect some atmospheric quantity X—can be estimated (*18*) for each of the two ensembles with the diagnostic Ω:

$$\Omega = (16\sigma^2_{<X>} - \sigma^2_X)/15\sigma^2_X \qquad (1)$$

where σ^2_X is the intraensemble variance of X and $\sigma^2_{<X>}$ is the corresponding variance of the ensemble-mean time series—the single time series generated by averaging across the 16 ensemble members at each time interval, chosen here to be 6 days. We are interested, of course, in precipitation; to reduce noise, however, we take X to be the natural logarithm of the precipitation. Performing statistics on the logarithms of precipitation is a common practice in hydrology and meteorology, because unmodified precipitation distributions tend to be highly skewed (*19*, *20*).

A study of the equation shows that outside of sampling error, Ω should vary from 0 to 1, with higher values implying a higher impact of the atmosphere's boundary conditions on precipitation. To isolate soil moisture's impact on precipitation from that of all other forcings, such as time-varying ocean temperatures and the seasonal variation of solar radiation, we compute the difference in the Ω values between the two ensembles. In simple terms, this Ω difference approximates the fraction of the precipitation variance explained by variations in soil moisture alone.

Figure 1 shows the global map of the Ω difference averaged across all of the participating models in GLACE. This multimodel estimation of land atmosphere coupling strength reveals several distinct hot spots. Hot spots appear in the central Great Plains of North America, the Sahel, equatorial Africa, and India. Less intense hot spots appear in South America, central Asia, and China.

The positions of the hot spots are not unexpected (*8*, *21*), particularly if the soil moisture influence is presumed to be local rather than remote. Consider first that in wet climates, for which soil water is plentiful, evaporation is controlled not by soil moisture but by net radiative energy. This is illustrated in Fig. 2, which shows how the Ω difference diagnostic, applied to evaporation rather than precipitation, varies (on average) with soil moisture. The Ω difference—the fraction of the evaporation variance explained by soil moisture variations—is indeed lowest when soil moisture is high. Because evaporation in wet climates is not highly sensitive to soil moisture variations, precipitation should not be sensitive to them, either.

Now consider that in dry climates, evaporation rates are sensitive to soil moisture but are also, of course, generally small, as demonstrated for the models by the dashed curve in Fig. 2. Intuitively, small evaporation rates should have a limited ability to affect precipitation. The atmosphere in dry regions is, in any case, predisposed to limit precipitation. Only in the transition zones between wet and dry climates, where the atmosphere is amenable to precipitation generation [in particular, where boundary-layer moisture can trigger moist convection (*22*)] and where evaporation is suitably high but still sensitive to soil moisture, can

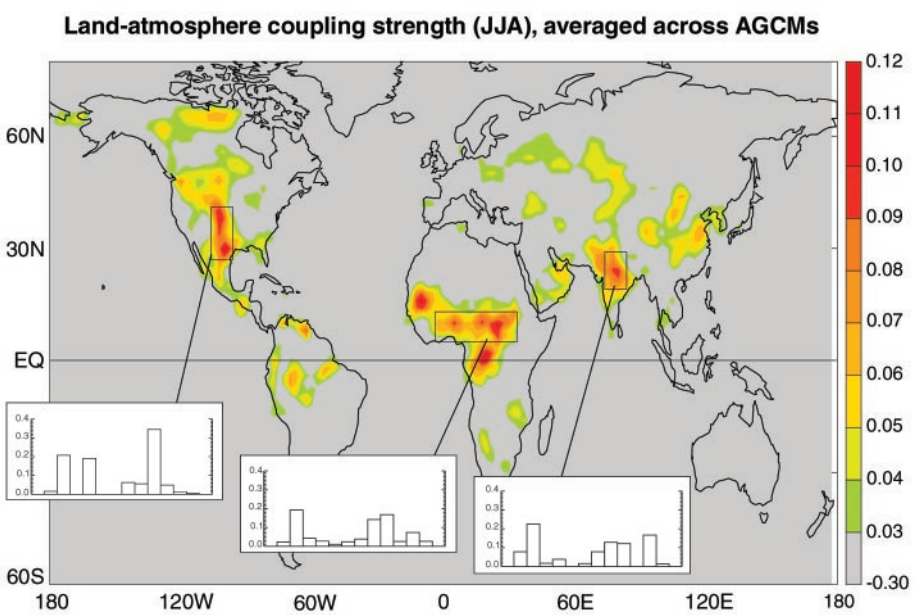

Fig. 1. The land-atmosphere coupling strength diagnostic for boreal summer (the Ω difference, dimensionless, describing the impact of soil moisture on precipitation), averaged across the 12 models participating in GLACE. (**Insets**) Areally averaged coupling strengths for the 12 individual models over the outlined, representative hotspot regions. No signal appears in southern South America or at the southern tip of Africa.

we expect soil moisture to influence precipitation. The major hot spots shown lie mainly in such transition zones (*23*).

The insets in the map (Fig. 1) show that not all of the GLACE models place hot spots in the regions indicated. In North America, for example, only half of the models show a statistically significant (*24*) coupling strength in the outlined region. The 12 models agree slightly more in the Sahelian and Indian hotspot regions; nevertheless, throughout the world, there exists extensive intermodel variability in the strength and positioning of the hot spots, a reflection of ongoing uncertainty in the proper way to represent the physical processes defining land-atmosphere coupling strength. Indeed, some of the models showing a small coupling strength in the insets also show a low coupling strength everywhere else on the planet. The intermodel variability highlights the importance of the averaging process leading to Fig. 1. The insets support the idea, stated above, that any single-model analysis of coupling strength will provide model-specific results. The patterns revealed by the averaging process are valuable because they show where many independent models agree that the land-atmosphere coupling is important.

The plotted hot spots indicate where a global initialization of soil moisture may enhance precipitation prediction skill during Northern Hemisphere summer (*25*, *26*). Under the assumption that the soil moisture impacts are predominantly local, the hot spots indicate where the routine monitoring of soil moisture, with both ground-based and space-based systems, will yield the greatest return in boreal summer seasonal forecasting. The hot spots are, in a sense, land-surface analogs to the ocean's "El Niño hot spot" in the eastern tropical Pacific.

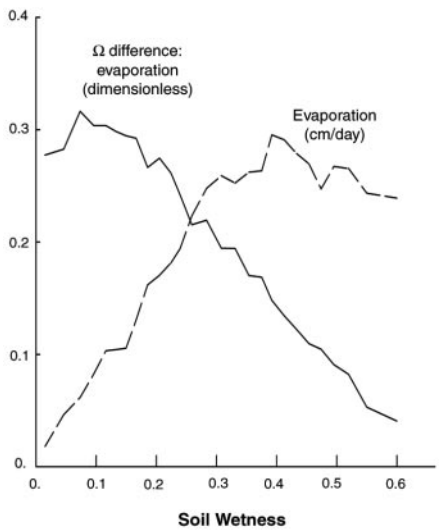

Fig. 2. Average relationship between soil wetness (the degree of saturation in the soil) and two separate aspects of the land-surface energy budget: the Ω difference for evaporation (solid curve, in dimensionless units) and the average evaporation rate (dashed curve, in cm/day). Both aspects should have suitably high values to allow soil moisture anomalies to be translated into precipitation anomalies; the plot shows that this mostly occurs for intermediate values of soil wetness, i.e., in the transition zones between wet and dry climates. The curves are derived by averaging the soil wetness, Ω difference, and evaporation fields across the 12 models, constructing scatter plots for the two relationships with data from nonice land points, and then binning the data according to soil wetness value.

References and Notes

1. J. M. Wallace *et al*., *J. Geophys. Res.* **103**, 14241 (1998).
2. B. P. Kirtman, P. S. Schopf, *J. Clim.* **11**, 2804 (1998).
3. E. M. Rasmusson, T. H. Carpenter, *Mon. Weather Rev.* **110**, 354 (1982).
4. Y. Vinnikov *et al*., *J. Geophys. Res.* **101**, 7163 (1996).
5. Historical soil moisture measurements are mostly confined to Asia (*27*). Even if global soil moisture fields did exist, using observations to establish that soil moisture affects precipitation is difficult because the other direction of causality is much stronger—precipitation has a first-order impact on soil moisture.
6. J. Shukla, Y. Mintz, *Science* **215**, 1498 (1982).
7. P. A. Dirmeyer, *J. Clim.* **13**, 2900 (2000).
8. R. D. Koster, M. J. Suarez, M. Heiser, *J. Hydrometeorol.* **1**, 26 (2000).
9. H. Douville, F. Chauvin, *Clim. Dyn.* **16**, 719 (2000).
10. P. A. Dirmeyer, *J. Hydrometeorol.* **4**, 329 (2001).
11. R. D. Koster, M. J. Suarez, *J. Hydrometeorol.* **4**, 408 (2003).
12. C. A. Schlosser, P. C. D. Milly, *J. Hydrometeorol.* **3**, 483 (2002).
13. C. M. Beljaars, P. Viterbo, M. J. Miller, A. K. Betts, *Mon. Weather Rev.* **124**, 362 (1996).
14. The participating AGCMs are from the following groups. (The order presented here is alphabetical and does not match the order of the histogram bars in Fig. 1.) (i) Bureau of Meteorology Research Centre (BMRC), Australia; (ii) The Canadian Center for Climate Modeling and Analysis (CCCma), Canada; (iii) Center for Climate System Research (CCSR), University of Tokyo, and National Institute for Environmental Studies (NIES), Japan; (iv) Center for Ocean-Land-Atmosphere Studies (COLA), United States; (v) Commonwealth Scientific and Industrial Research Organization (CSIRO), Australia; (vi) NASA/Goddard Space Flight Center Laboratory for Atmospheres, Climate and Radiation Branch, United States (GEOS); (vii) Geophysical Fluid Dynamics Laboratory (GFDL), United States; (viii) Hadley Center (HadAM3), UK; (ix) National Center for Atmospheric Research (NCAR), United States; (x) National Center for Environmental Prediction (NCEP), United States; (xi) NASA Seasonal-to-Interannual Prediction Project [now part of the Global Modeling and Assimilation Office (GMAO)], United States; and (xiii) University of California, Los Angeles (UCLA).
15. GLACE is a joint project of the Global Energy and Water Cycle Experiment (GEWEX) Global Land Atmosphere System Study (GLASS) and the Climate Variability Experiment (CLIVAR) Working Group on Seasonal-to-Interannual Prediction (WGSIP), all under the aegis of the World Climate Research Programme (WCRP).
16. Coupling strength in this report refers to the general ability of land surface moisture anomalies—either local or remote—to affect precipitation in a given region. Inferences regarding soil moisture measurement in the indicated hot spots require an assumption of local influence.
17. The prescribed soil moistures necessarily differed from model to model, because each time series had to be fully consistent with the individual model using it. The prescribed moistures for a given model came, in fact, from one of the model's simulations in the first, "variable soil moisture" ensemble. In GLACE, subsurface moisture refers to a soil moisture prognostic variable having an assigned effective depth of more than 5 cm from the surface. Soil moistures corresponding to shallower depths are not reset in the experiment. For details, see the experiment plan posted on the GLACE Web site: http://glace.gsfc.nasa.gov/.
18. R. D. Koster *et al*., *J. Hydrometeorol.* **3**, 363 (2002).
19. G. Drufuca, I. I. Zawadzki, *J. Appl. Meteorol.* **14**, 1419 (1975).
20. B. Kedem, L. S. Chiu, G. R. North, *J. Geophys. Res.* **95**, 1965 (1990).
21. Indirect (and thus limited in its own right) observational estimates (*28*) of the North American hot spot roughly agree with that shown in the figure.
22. Y. C. Sud, W. C. Chao, G. K. Walker, *J. Arid Environ.* **25**, 5 (1993).
23. Neither equatorial Africa nor the northernmost reaches of Canada are traditionally considered transition zones between wet and arid climates, and the appearance of hot spots in these regions is not so easily explained. On average, the models do show a pronounced sensitivity of evaporation to soil moisture in equatorial Africa, belying its intuitive status as an atmosphere-controlled evaporation regime.
24. For a single model at a single grid cell, an Ω difference of 0.06 is significant at the 95% confidence level. If the grid cells within a region are completely independent, then a regional (averaged over, say, 10 grid cells) Ω difference of 0.002 is significant at the 95% confidence level. The actual 95% confidence value for the bars in the histograms lies somewhere between these two values, because although multiple grid cells contribute to the regional average, the grid cells are not fully independent. A single exact value cannot be computed, because each AGCM uses its own horizontal grid resolution and simulates unique spatial correlation structures.
25. This study has focused on soil moisture effects alone. Vegetation properties and processes also have substantial impacts on climate in a number of regions. For example, Charney *et al*. (*29*) describe the importance of surface albedo on North American climate; Dickinson and Henderson-Sellers (*30*) show the impact of deforestation on Amazonian climate; and Xue *et al*. (*31*) demonstrate the importance of vegetation processes on east Asian climate. This issue, like the soil moisture issue, is a subject of continuing investigation.
26. The relative importance of sea surface temperature (SST) forcing in the indicated hot spots cannot be determined in this experiment, for two reasons. (i) The SST signal in either of the two ensembles cannot be separated from the strong seasonality signal associated with the Sun's transit across the sky over the 3-month simulation period. (ii) Only a single year of SSTs is prescribed, so the effect of interannually varying SSTs is not captured. As noted in the text, some studies (*8*) show a strong SST impact in the tropics and subtropics (encompassing the indicated hot spots in Africa and southern Asia) and a relatively weak impact in midlatitudes (encompassing the North American hot spot).
27. A. Robock *et al*., *Bull. Am. Meteorol. Soc.* **81**, 1281 (2000).
28. R. D. Koster, M. J. Suarez, R. W. Higgins, H. M. Van den Dool, *Geophys. Res. Lett.* **30**, 1241, 10.1029/2002GL016571 (2003).
29. J. Charney, W. J. Quirk, S. H. Chow, J. Kornfield, *J. Atmos. Sci.* **34**, 1366 (1977).
30. R. E. Dickinson, A. Henderson-Sellers, *Q. J. R. Meteorol. Soc.* **114**, 439 (1988).
31. Y. K. Xue *et al*., *J. Geophys. Res.* **109**, D03105, 10.1029/2003JD003556 (2004).

32. We thank the listed institutions for the computational support needed to perform the simulations. We also thank M. Kistler for help with the GLACE project Web page and T. Bell for statistical advice.

12 May 2004; accepted 7 July 2004